Inorg. Chem. **2004**, *43*, 8092–8101

Comparative Kinetics and Mechanism of Oxygen and Sulfur Atom Transfer Reactions Mediated by Bis(dithiolene) Complexes of Molybdenum and Tungsten

Jun-Jieh Wang,[†] Olga P. Kryatova,[‡] Elena V. Rybak-Akimova,[‡] and R. H. Holm[†,*]

Department of Chemistry and Chemical Biology, Harvard University, Cambridge, Massachusetts 02138, and Department of Chemistry, Tufts University, Medford, Massachusetts 02155

Received June 30, 2004

Although the kinetics and mechanism of metal-mediated oxygen atom (oxo) transfer reactions have been examined in some detail, sulfur atom (sulfido) transfer reactions have not been similarly scrutinized. The reactions $[M^{IV}(O\text{-}p\text{-}C_6H_4X')(S_2C_2Me_2)_2]^{1-} + Ph_3AsQ \rightarrow [M^{VI}Q(O\text{-}p\text{-}C_6H_4X')(S_2C_2Me_2)_2]^{1-} + Ph_3As$ (M = Mo, W; Q = O, S) with variable substituent X′ have been investigated in acetonitrile in order to determine the relative rates of oxo versus sulfido transfer at constant structure (square pyramidal) of the atom acceptor and of atom transfer at constant structure of the atom donor and metal variability of the atom acceptor. All reactions exhibit second-order kinetics and entropies of activation (–25 to –45 eu) consistent with an associative transition state. At parity of atom acceptor, k_2^S (0.25–0.75 $M^{-1}s^{-1}$) > k_2^O (0.023–0.060 $M^{-1}s^{-1}$) with M = Mo and k_2^S (4.1–66.7 $M^{-1}s^{-1}$) > k_2^O (1.8–9.8 $M^{-1}s^{-1}$) with M = W. At constant atom donor and X′, $k_2^W > k_2^{Mo}$ with reactivity ratios k_2^W/k_2^{Mo} = 78–184 (Q = O) and 16–89 (Q = S). Rate constants refer to 298 K. At constant M and Q, rates increase in the order X′ = Me $\lesssim$ OMe < H < Br < COMe < CN; increasing electron-withdrawing propensity accelerates reaction rates. The probable transition state involves significant $Ph_3AsQ\cdots M$ bond-making (X′ rate trend) and concomitant As–Q bond weakening (bond energy order As–O > As–S). Orders of oxo and sulfido donor ability of substrates and complexes are deduced on the basis of qualitative reactivity properties determined here and elsewhere. This work complements previous studies of the reaction systems $[M^{IV}(O\text{-}p\text{-}C_6H_4X')(S_2C_2Me_2)_2]^{1-}$/XO where the substrates are N-oxides and S-oxides and $k_2^W > k_2^{Mo}$ at constant substrate also applies. The reaction order of substrates is $Me_3NO > (CH_2)_4SO > Ph_3AsS > Ph_3AsO$. This research provides the first quantitative information of metal-mediated sulfido transfer.

Introduction

We have recently developed analogue reaction systems of the molybdenum and tungsten oxotransferases based on the minimal oxygen atom transfer reaction 1 with M = Mo and W and oxo donors XO = N-oxides and S-oxides.[1−3] The reactant complexes are square pyramidal bis(dithiolenes) of the general type $[M^{IV}(OR')(S_2C_2R_2)_2]^{1-}$ (R′ = p-C_6H_4X'; R = Me, Ph), which convert to the distorted octahedral products $[M^{VI}O(OR')(S_2C_2R_2)_2]^{1-}$ and afford products X = amines and sulfides. Reactions in tungsten-based systems in particular are clean and complete. Kinetics data and mechanistic considerations reduce to second-order reactions proceeding through an associative transition state with substantial M···OX bond-making character. The leading aspects of this research are summarized elsewhere.[4]

$$M^{IV} + XO \rightarrow M^{VI}O + X \qquad (1)$$

Of all metal-mediated atom and group transfer reactions, oxo transfer is by far the most extensively documented and throughly investigated. Reaction 1 is merely one example of a manifold of transformations which proceed by primary oxo transfer (i.e., reactions in which reactants XO/X are

* Author to whom correspondence should be addressed. E-mail: holm@chemistry.harvard.edu.
[†] Harvard University.
[‡] Tufts University.

(1) Lim, B. S.; Holm, R. H. *J. Am. Chem. Soc.* **2001**, *123*, 1920−1930.
(2) Sung, K.-M.; Holm, R. H. *J. Am. Chem. Soc.* **2001**, *123*, 1931−1943.
(3) Sung, K.-M.; Holm, R. H. *J. Am. Chem. Soc.* **2002**, *124*, 4312−4320.
(4) Enemark, J. H.; Cooney, J. J. A.; Wang, J.-J.; Holm, R. H. *Chem. Rev.* **2004**, *104*, 1175−1200.

10.1021/ic040087f CCC: $27.50
Published on Web 11/17/2004

single oxygen atom donors/acceptors, the oxidation state change $M^{z/z+2}$ results from atom transfer only, and the transferable or transferred atom is oxidic and bound in a terminal or bridging mode directly to atom M).[5] The situation may be contrasted with primary sulfur atom transfer reactions with analogous defining features and whose relatively few examples can be summarized by the minimal reactions 2−6. The first three are sulfido transfer from substrate resulting in the formation of M═S units, while the last two are sulfido transfer to substrate with concomitant metal reduction. Frequently used sulfur acceptors X are R_3P and CN^-, and sulfur donors XS are elemental sulfur, episulfides, RNCS, RSSSR, or a M═S complex. (The reaction types do not include MS_n species ($n \geq 2$), many of which function as sulfur atom donors.)

$$M^{II} + XS \rightarrow M^{IV}S + X \quad (2)$$
$$M = Ti,[6]\ Mo,[7,8]\ W,[7-9]\ Sn[10-12]$$

$$M^{IV} + XS \rightarrow M^{VI}S + X \quad (3)$$
$$M = W[13-15]$$

$$M^{IV}O + XS \rightarrow M^{VI}O(S) + X \quad (4)$$
$$M = Mo[16-18]$$

$$M^{VI}O(S) + X \rightarrow M^{IV}O + XS \quad (5)$$
$$M = Mo,[18-21]\ W[22]$$

$$M^{VI}S_2 + X \rightarrow M^{IV}S + XS \quad (6)$$
$$M = W[22,23]$$

During our examination of the reactivity of bis(dithiolene)-W^{IV} complexes, we observed several instances of sulfur atom transfer reaction 3 with $XS = (PhCH_2S)_2S$ and oxo transfer reaction 1 with $XO = Ph_3AsO$.[2,15] The latter reagent has previously been effective in a molybdenum-mediated non-dithiolene reaction system.[24,25] More recent experimentation has led to reactions 7 and 8 with M = Mo and W. These are specific examples of reactions 1 and 3, respectively, and are set out in detail in Figure 1. The compound Ph_3AsS has been shown to be a sulfur donor to other group 15 compounds in

$$[M^{IV}(O\text{-}p\text{-}C_6H_4X)(S_2C_2Me_2)_2]^{1-} + Ph_3AsO \rightarrow [M^{VI}O(O\text{-}p\text{-}C_6H_4X)(S_2C_2Me_2)_2]^{1-} + Ph_3As \quad (7)$$

$$[M^{IV}(O\text{-}p\text{-}C_6H_4X)(S_2C_2Me_2)_2]^{1-} + Ph_3AsS \rightarrow [M^{VI}S(O\text{-}p\text{-}C_6H_4X)(S_2C_2Me_2)_2]^{1-} + Ph_3As \quad (8)$$

reactions for which limited kinetics and thermodynamic data are available.[26−28] It has apparently not been utilized previously in metal-mediated sulfido transfer reactions. Reactions 7 and 8 provide an opportunity to determine (i) the relative rates of oxo versus sulfido transfer at constant structure of the atom acceptor (Mo^{IV} or W^{IV}) and nearly constant structure of the atom donor, and (ii) the relative rates of atom transfer at constant structure of the atom donor and metal variability of the atom acceptor. There have been no previous determinations of the kinetics and mechanism of sulfur atom transfer. Consequently, ii is a matter of interest in its own right and also because of the existence of polysulfide reductase. This molybdoenzyme has been classified in the dimethyl sulfoxide (DMSO) reductase family; hence its active site is very likely of the bis(dithiolene) type.[29] Additionally, we are interested in analogue reaction systems of arsenite oxidase, which converts arsenite ($H_2AsO_3^-$) to arsenate ($HAsO_4^{2-}$).[30,31] There is very little information on oxo transfer reactions of arsenic compounds, a matter redressed to an extent by the reactivity demonstrated here between Ph_3AsO and Mo^{IV} and W^{IV} dithiolenes.

Experimental Section

Preparation of Compounds. All reactions and manipulations were conducted under a pure dinitrogen atmosphere using either an inert atmosphere box or standard Schlenk techniques. Methanol was distilled from magnesium; acetonitrile, ether, dichloromethane, and tetrahydrofuran (THF) were freshly purified using an Innovative Technology solvent purification system and stored over 4-Å molecular sieves. Benzene and *n*-pentane used in column chromatography were of HPLC grade from J. T. Baker. Deuterated solvents (Cambridge Isotope Laboratories, Inc.) were stored over molecular sieves under dinitrogen. Commercial samples (Aldrich) of the compounds Ph_3AsO, Ph_3SbS, and As_2O_3 were sublimed and $(EtO)_3$-As was distilled prior to use. Ph_3AsS was obtained by the reaction of Ph_3AsO with $(Me_3Si)_2S$ in acetonitrile in ≳90% yield, and NaO-

(5) Holm, R. H. *Chem. Rev.* **1987**, *87*, 1401−1449.
(6) Woo, L. K. *Chem. Rev.* **1993**, *93*, 1125−1136.
(7) Hall, K. A.; Mayer, J. M. *J. Am. Chem. Soc.* **1992**, *114*, 10402−10411.
(8) Hall, K. A.; Mayer, J. M. *Inorg. Chem.* **1994**, *33*, 3289−3298.
(9) Su, F.-M.; Bryan, J. C.; Jang, S.; Mayer, J. M. *Polyhedron* **1989**, *8*, 1261−1277.
(10) Guilard, R.; Ratti, C.; Barbe, J.-M.; Dubois, D.; Kadish, K. M. *Inorg. Chem.* **1991**, *30*, 1537−1542.
(11) Kuchta, M.; Parkin, G. *J. Am. Chem. Soc.* **1994**, *116*, 8372−8373.
(12) Berreau, L. M.; Woo, L. K. *J. Am. Chem. Soc.* **1995**, *117*, 1314−1317.
(13) Lorber, C.; Donahue, J. P.; Goddard, C. A.; Nordlander, E.; Holm, R. H. *J. Am. Chem. Soc.* **1998**, *120*, 8102−8112.
(14) Sung, K.-M.; Holm, R. H. *Inorg. Chem.* **2001**, *40*, 4518−4525.
(15) Jiang, J.; Holm, R. H. *Inorg. Chem.* **2004**, *43*, 1302−1310.
(16) Eagle, A. A.; Laughlin, L. J.; Young, C. G.; Tiekink, E. R. T. *J. Am. Chem. Soc.* **1992**, *114*, 9195−9197.
(17) Young, C. G.; Laughlin, L. J.; Colmanet, S.; Scrofani, S. D. B. *Inorg. Chem.* **1996**, *35*, 5368−5377.
(18) Smith, P. D.; Slizys, D. A.; George, G. N.; Young, C. G. *J. Am. Chem. Soc.* **2000**, *122*, 2946−2947.
(19) Thapper, A.; Donahue, J. P.; Musgrave, K. B.; Willer, M. W.; Nordlander, E.; Hedman, B.; Hodgson, K. O.; Holm, R. H. *Inorg. Chem.* **1999**, *38*, 4104−4114.
(20) Adam, W.; Bargon, R. M.; Schenk, W. A. *J. Am. Chem. Soc.* **2003**, *125*, 3871−3876.
(21) Adam, W.; Bargon, R. M. *Chem. Rev.* **2004**, *104*, 251−261.
(22) Eagle, A. A.; Gable, R. W.; Thomas, S.; Sproules, S. A.; Young, C. G. *Polyhedron* **2004**, *23*, 385−394.
(23) Eagle, A. A.; Tiekink, E. R. T.; George, G. N.; Young, C. G. *Inorg. Chem.* **2001**, *40*, 4563−4573.
(24) Schultz, B. E.; Gheller, S. F.; Muetterties, M. C.; Scott, M. J.; Holm, R. H. *J. Am. Chem. Soc.* **1993**, *115*, 2714−2722.
(25) Schultz, B. E.; Holm, R. H. *Inorg. Chem.* **1993**, *32*, 4244−4248.
(26) Baechler, R. D.; Stack, M.; Stevenson, K.; Van Valkenburgh, V. *Phosphorus, Sulfur Silicon Relat. Elem.* **1990**, *48*, 49−52.
(27) Jason, M. E. *Inorg. Chem.* **1997**, *36*, 2641−2646.
(28) Capps, K. B.; Wixmerten, B.; Bauer, A.; Hoff, C. D. *Inorg. Chem.* **1998**, *37*, 2861−2864.
(29) Hille, R. *Chem. Rev.* **1996**, *96*, 2757−2816.
(30) Anderson, G. L.; Williams, J.; Hille, R. *J. Biol. Chem.* **1992**, *267*, 23674−23682.
(31) Ellis, P. J.; Conrads, T.; Hille, R.; Kuhn, P. *Structure* **2001**, *9*, 125−132.

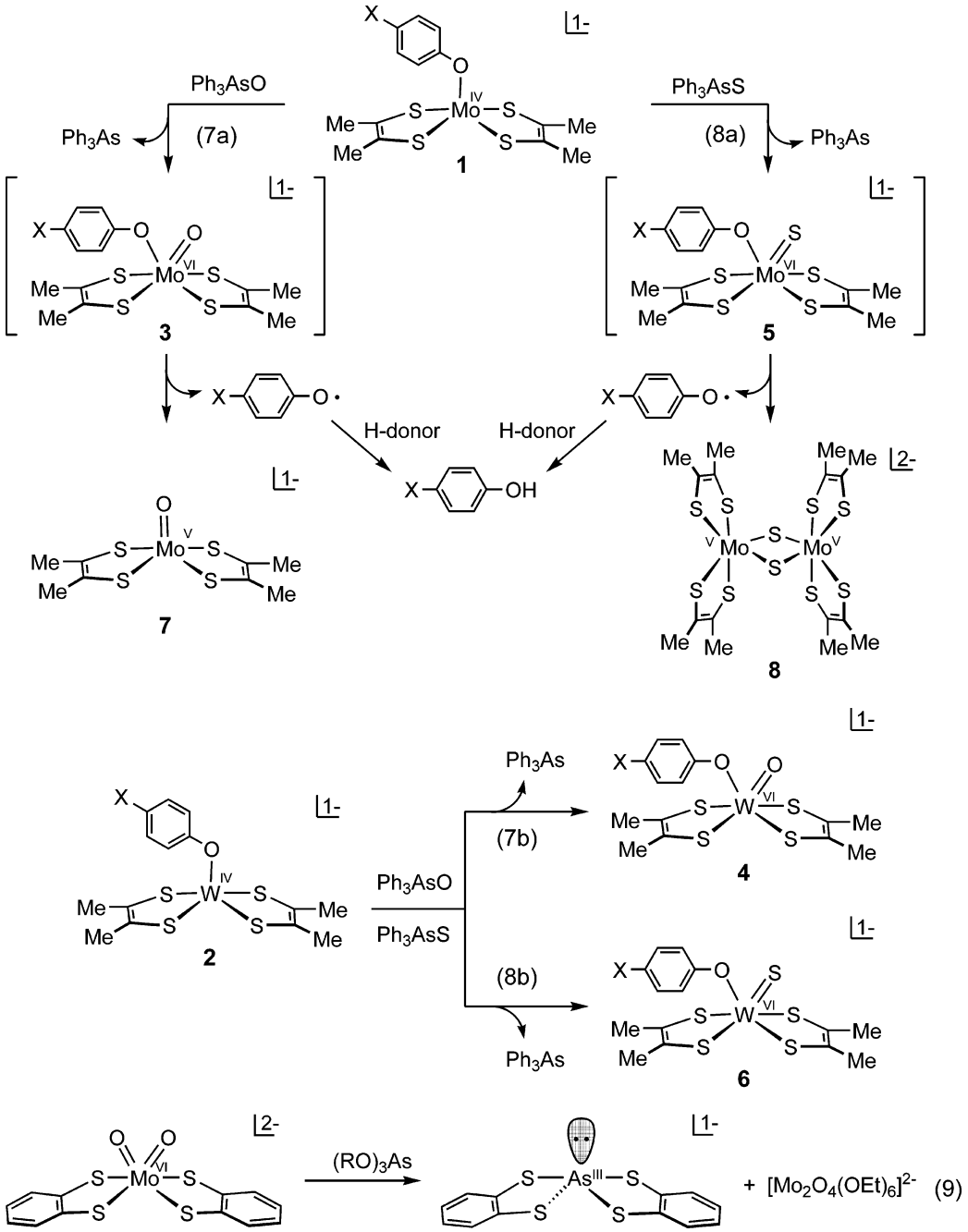

Figure 1. Schematic depiction of the atom transfer reactions of bis(dithiolene)M(IV) complexes **1** and **2**, including oxo transfer (reactions 7a and 7b) and sulfido transfer (reactions 8a and 8b). The structures of product oxo (**3**, **4**) and sulfido (**6**) complexes have been established in previous work. Complex **5** is unstable to internal redox and decays to **8** in solution. Reaction 9 shows the ligand transfer reaction between a $Mo^{VI}O_2$ complex and arsenite esters.

p-C_6H_4X' was prepared from addition of 1 equiv of NaOMe to *p*-X′-C_6H_4OH (X′ = H, Me, OMe, Br, COMe, CN) in methanol. In the following preparations, all volume reduction steps were performed in vacuo.

1-Methyl-4-arsa-3,5,8-trioxabicyclo[2.2.2]octane. The following method is more convenient and leads to higher yields than the published procedure.[32] Arsenic trioxide (9.9 g, 50 mmol) and 2-hydroxymethyl-2-methyl-1,3-propanediol 12.0 g (100 mmol) were covered with toluene (100 mL) and refluxed for 10 h. A Dean-Stark trap was used to collect water generated during the reaction. The solvent was removed; the solid residue was sublimed to give the product as 8.20 g (85%) of hygroscopic colorless crystals; mp 42 °C, lit.[32] 41−42°. ^{1}H NMR (CD_3CN): δ 0.63 (s, 1), 4.02 (s, 2).

4-Arsa-3,5,7-trioxabicyclo[2.2.1]heptane. The following procedure is related to a published method.[33] A mixture of As_2O_3 (9.9 g, 50 mmol), glycerol (9.2 g, 100 mmol), and toluene (100 mL) was refluxed for 8 h, resulting in a colorless, very viscous syrup. The crude product was sublimed and the sublimate was resublimed, giving the product as 2.7 g (33%) of extremely hygroscopic crystals; mp 69 °C, lit.[33] 66−70 °C. ^{1}H NMR (CD_3CN): δ 5.15 (t, 1), 3.88 (m, 2), 3.55 (m, 2).

$(Et_4N)[As(bdt)_2]$. A solution of $(Et_4N)_2[MoO_2(bdt)_2]$[34] (20 mg, 0.032 mmol; bdt = benzene-1,2-dithiolate(2-)) in 1 mL of acetonitrile was treated with a solution of $(EtO)_3As$ (20 mg, 0.095 mmol)

(32) Verkade, J. G.; Reynolds, L. T. *J. Org. Chem.* **1960**, *25*, 663−665.

(33) Wolfrom, M. L.; Holm, M. J. *J. Org. Chem.* **1961**, *26*, 273−274.

(34) Ueyama, N.; Oku, H.; Kondo, M.; Okamura, T.; Yoshinaga, N.; Nakamura, A. *Inorg. Chem.* **1996**, *35*, 643−650.

in 1 mL of acetonitrile. The light yellow solution was stirred for 3 h and filtered. The filtrate was reduced to one-third of its original volume. Several volume equivalents of ether were layered onto the solution, and the mixture was allowed to stand overnight. The product was collected, washed with ether, and obtained as 4.0 mg (26%) of colorless crystals. ^{1}H NMR (CD_3CN, anion): δ 6.79 (m, 2), 7.14 (q, 2). The compound was identified by an X-ray structure determination.

$(Et_4N)[Mo(O\text{-}p\text{-}C_6H_4X')(S_2C_2Me_2)_2]$. These compounds were prepared in an analogous procedure for $[Mo(OPh)(S_2C_2Me_2)_2]^{1-}$ [1] with NaO-p-C_6H_4X' instead of NaOPh on a 0.16−0.22 mmol scale. A suspension of NaO-p-C_6H_4X' in acetonitrile was added to a suspension of 1 equiv of $[Mo(CO)_2(S_2C_2Me_2)_2]$[35] in acetonitrile. The mixture was stirred for 6−8 h to generate a brown or green-brown solution. A solution of 1 equiv of Et_4NCl in acetonitrile was added; the mixture was stirred for 10 min and filtered. The filtrate was reduced to one-third of its original volume, several volume equivalents of ether were layered onto the solution, and the mixture was allowed to stand for 2 days. All compounds were isolated as highly crystalline solids; yields are indicated

X′ = Me. Brown needle-shaped crystals (56%). ^{1}H NMR (CD_3CN, anion): δ 2.14 (s, 3), 2.57 (s, 12), 6.27 (d, 2), 6.80 (d, 2). Absorption spectrum (acetonitrile) λ_{max} (ϵ_M): 272 (sh, 13 400), 344 (12 050), 392 (3600), 473 (1470), 571 (sh, 430), 736 (120) nm.

X′ = OMe. Brown needle-shaped crystals (52%). ^{1}H NMR (CD_3CN, anion): δ 2.57 (s, 12), 3.61 (s, 3), 6.32 (d, 2), 6.55 (d, 2). Absorption spectrum (acetonitrile) λ_{max} (ϵ_M): 274 (sh, 13 000), 344 (12 000), 389 (4100), 466 (1750), 570 (sh, 490), 737 (210) nm.

X′ = Br. Dark-orange block-shaped crystals (32%). ^{1}H NMR (CD_3CN, anion): δ 2.59 (s, 12), 6.30 (d, 2), 7.11 (d, 2). Absorption spectrum (acetonitrile): λ_{max} (ϵ_M): 272 (sh, 12 400), 340 (11 050), 396 (3400), 468 (1500), 570 (sh, 465), 730 (150) nm.

X′ = COMe. Green-brown block-shaped crystals (20%). ^{1}H NMR (CD_3CN, anion): δ 2.42 (s, 3), 2.60 (s, 12), 6.42 (d, 2), 7.64 (d, 2). Absorption spectrum (acetonitrile) λ_{max} (ϵ_M): 272 (sh, 13 800), 338 (12 900), 393 (3650), 463 (1250), 571 (sh, 385), 735 (115) nm.

$(Et_4N)[W(O\text{-}p\text{-}C_6H_4COMe)(S_2C_2Me_2)_2]$. The compound was prepared in an analogous procedure for $(Et_4N)[W(O\text{-}p\text{-}C_6H_4X')(S_2C_2Me_2)_2]^{1-}$ [3] with use of $[W(CO)_2(S_2C_2Me_2)_2]$[36] and NaO-p-C_6H_4-COMe. The reaction was conducted on a 0.25 mmol scale in THF. After the addition of 1 equiv of Et_4NCl, the reaction mixture was stirred for 10 min. The dark green-brown residue after solvent removal was dissolved in 1 mL of acetonitrile, and the solution was filtered. Ether (15 mL) was layered onto the filtrate, causing the separation of dark green-brown block-shaped crystals over 1 day, which were dried to afford the product (40%). ^{1}H NMR (CD_3CN, anion): δ 2.44 (s, 3), 2.67 (s, 12), 6.50 (d, 2), 7.67 (d, 2). Absorption spectrum (acetonitrile): λ_{max} (ϵ_M) 282 (sh, 14 500), 297 (15 400), 323 (sh, 8900), 404 (sh, 2500), 485 (sh, 900), 654 (600) nm.

$(Et_4N)[WS(O\text{-}p\text{-}C_6H_4X')(S_2C_2Me_2)_2]$. These compounds were formed in situ by the immediate and complete reaction of $[W(O\text{-}p\text{-}C_6H_4X')(S_2C_2Me_2)_2]^{1-}$ (7.1−7.6 mmol) with 2.0 equiv of Ph_3AsS in CD_3CN; reactions were monitored by ^{1}H NMR spectroscopy. Product solutions are dark red-brown; methyl chemical shifts (δ 2.27−2.35) overlap that of $[WS(OPh)(S_2C_2Me_2)_2]^{1-}$ (δ 2.29).[14] **X′ = Me**: δ 2.27 (s, 3), 2.32 (s, 12), 6.86 (d, 2), 7.03 (d, 2). **X′ = OMe**: δ 2.31 (s, 12), 3.76 (s, 3), 6.79 (d, 2), 6.91 (d, 2). **X′ = Br**: δ 2.33 (s, 12), 6.90 (d, 2), 7.31 (d, 2). **X′ = COMe**: δ 2.34 (s, 12), 2.49 (s, 3), 7.02 (d, 2), 7.86 (d, 2). **X′ = CN**: δ 2.35 (s, 12), 7.06 (d, 2), 7.46 (d, 2).

Table 1. Crystallographic Data for $(Et_4N)[As(bdt)_2]$[a]

formula	$C_{20}H_{28}AsNS_4$	β, deg	106.91(1)
fw	485.59	Z	4
crystal system	monoclinic	V, Å^3	2220(3)
space group	$P2_1/c$	d_{calc}, g/cm^3	1.453
T, K	213	μ, mm^{-1}	1.912
a, Å	10.462(8)	θ range, deg	1.98−22.50
b, Å	14.103(10)	GOF (F^2)	1.277
c, Å	15.730(11)	R_1 [b] (wR_2 [c])	5.25 (8.32)

[a] Mo Kα radiation (λ = 0.71073 Å). [b] $R_1 = \sum||F_o| - |F_c||/\sum|F_o|$. [c] $wR_2 = \{\sum[w(F_o^2 - F_c^2)]^2/\sum[w(F_o^2)^2]\}^{1/2}$.

X-ray Structure Determination. The structure of the compound in Table 1 was determined. Single crystals were obtained by layering several volume equivalents of ether onto an acetonitrile solution and allowing the mixture to stand for at least 12 h. A crystal was mounted on a Siemens (Bruker) SMART CCD-based diffractometer. Data were collected at 213 K using Mo Kα radiation (λ = 0.71073 D) and ω scans of 0.3°/frame for 30 s, such that 1271 frames were collected for a hemisphere of data. The first 50 frames were recollected at the end of the data collection to monitor for decay; no significant decay was detected. Cell parameters were retrieved using SMART software and refined using SAINT software. Data reduction was performed with SAINT; absorption corrections were applied with SADABS. The space group was assigned from analysis of symmetry and systematic absences using XPREP. The structure was solved by direct methods and refined by full-matrix least-squares method against F^2 using SHELXL-97. All non-hydrogen atoms were refined anisotropically; hydrogen atoms were placed at idealized positions of carbon atoms. Crystal data and final agreement factors are given in Table 1.[37]

Kinetics Measurements. Sample preparations and reactions were performed under strictly anaerobic conditions in acetonitrile or dimethylformamide (DMF) solutions. The reaction systems $(Et_4N)[M(O\text{-}p\text{-}C_6H_4X')(S_2C_2Me_2)_2]/Ph_3AsO$ (M = Mo, W) and $(Et_4N)[Mo(O\text{-}p\text{-}C_6H_4X')(S_2C_2Me_2)_2]/Ph_3AsS$ or Ph_3SbS were conventionally monitored with a Varian Cary 3 spectrophotometer equipped with a cell compartment thermostated to ±0.5 K. Thermal equilibrium was reached by placing a quartz cell (1 mm path length) containing 0.28-mL solutions of the complexes in the cell compartment at least 5 min prior to reaction initiation. Reactions were initiated by the injection of substrate (in acetonitrile or DMF solutions) using a gastight syringe (100 μL) through the rubber septum cap of the quartz cell followed by rapid shaking of the solution mixtures. The following initial concentrations were used: $[Mo^{IV}]_0$ = 1.76−2.14 mM, $[Ph_3AsO]_0$ = 14.3−29.4 mM; $[Mo^{IV}]_0$ = 0.88−1.07 mM, $[Ph_3AsS]_0$ = 2.86−5.88 mM; $[W^{IV}]_0$ = 1.50−1.85 mM, $[Ph_3AsO]_0$ = 7.69−25.0 mM. Tight isosbestic points occurred in each reaction system, demonstrating clean conversions. For each substrate, reactions were conducted at five temperatures in the range of 278−333 K. At each temperature, at least five independent runs with different initial concentrations $[Ph_3AsO]_0$ were performed under pseudo-first-order conditions for molybdenum and tungsten complexes. Plots of $\ln[(A_t - A_\infty)/(A_0 - A_\infty)]$ versus time were linear over at least 3 half-lives, and the initial rate constants k_{obs} were obtained from the data for the first 30 min. Plots of k_{obs} versus $[Ph_3AsO]_0$ were linear and yielded overall

(35) Lim, B. S.; Donahue, J. P.; Holm, R. H. *Inorg. Chem.* **2000**, *39*, 263−273.
(36) Goddard, C. A.; Holm, R. H. *Inorg. Chem.* **1999**, *38*, 5389−5398.

(37) See paragraph at the end of this article for Supporting Information available.

Chart 1. Designation of Complexes

$[Mo^{IV}(O\text{-}p\text{-}C_6H_4X')(S_2C_2Me_2)_2]^{1-}$
X′ = H **1a**,[1,39] Me **1b**, OMe **1c**, Br **1d**, COMe **1e**
$[W^{IV}(O\text{-}p\text{-}C_6H_4X')(S_2C_2Me_2)_2]^{1-}$ [3,40]
X′ = H **2a**, Me **2b**, OMe **2c**, Br **2d**, COMe **2e**, CN **2f**
$[Mo^{VI}O(O\text{-}p\text{-}C_6H_4X')(S_2C_2Me_2)_2]^{1-}$
X′ = H **3a**, Me **3b**, OMe **3c**, Br **3d**, COMe **3e**
$[W^{VI}O(O\text{-}p\text{-}C_6H_4X')(S_2C_2Me_2)_2]^{1-}$ [3,39]
X′ = H **4a**, Me **4b**, OMe **4c**, Br **4d**, COMe **4e**, CN **4f**
$[Mo^{VI}S(O\text{-}p\text{-}C_6H_4X')(S_2C_2Me_2)_2]^{1-}$
X′ = H **5a**, Me **5b**, OMe **5c**, Br **5d**, COMe **5e**
$[W^{VI}S(O\text{-}p\text{-}C_6H_4X')(S_2C_2Me_2)_2]^{1-}$
X′ = H **6a**,[14] Me **6b**, OMe **6c**, Br **6d**, COMe **6e**, CN **6f**
$[Mo^{V}O(S_2C_2Me_2)_2]^{1-}$ **7**[35]
$[Mo^{V}_2S_2(S_2C_2Me_2)_4]^{2-}$ **8**[35]

second-order rate constants k_2 at each temperature. In case of mixed-second-order conditions for the sulfido transfer reactions to molybdenum complexes, at each temperature at least five independent runs with different initial concentrations $[Ph_3AsS]_0$ were performed. The second-order rate constants k_2 (M^{-1} s^{-1}) were obtained from the plots of $\{\ln([Ph_3AsS]_t/[Mo^{IV}]_t) - \ln([Ph_3AsS]_0/[Mo^{IV}]_0)\}/([Ph_3AsS]_0 - [Mo^{IV}]_0)$ versus time, in which the values of $[Mo^{IV}]_t$ and $[Ph_3AsS]_t$ were calculated from the equations of $[Mo^{IV}]_t = [Mo^{IV}]_0 - (A_t - A_0)/(A_\infty - A_0)[Mo^{IV}]_0$ and $[Ph_3AsS]_t = [Ph_3AsS]_0 - (A_t - A_0)/(A_\infty - A_0)[Mo^{IV}]_0$, respectively. Rate constants k_2 were averaged from the values which were obtained from multiple independent runs.[38]

Because of faster reaction rates, the systems $(Et_4N)[W(O\text{-}p\text{-}C_6H_4X')(S_2C_2Me_2)_2]/Ph_3AsS$ were investigated using a Hi-Tech Scientific (Salisbury, Wilshire, UK) SF-43 Multi-Mixing Cryo-Stopped-Flow instrument in a diode array mode. The instrument was equipped with stainless steel plumbing, a stainless steel mixing chamber with sapphire windows, and an anaerobic gas-flushing kit. The temperature in the mixing cell (1 cm) was maintained to ±0.1 K, and the mixing time was 2−3 ms. Experiments were performed in a single-mixing mode of the instrument. Reactions were studied under second-order conditions within the 0.25−0.75 mM concentration range of complex and substrate (after mixing) at 293−323 K (283−323 K for X′ = CN). A series of four to six shots at each temperature gave standard deviations within 10%. Data analysis was performed with IS-2 Rapid Kinetic (Hi-Tech) and Spectfit/32 Global Analysis System (Spectrum Software) software with the relationship $A_t = A_\infty - (A_\infty - A_0)/(1 + k_2C)$, where C is the concentration of reagents under equimolar conditions. Activation parameters were determined from plots of the Eyring equation $k = (k_BT/h)[\exp(\Delta S^{\ddagger}/R - \Delta^{\ddagger}H/RT)]$. Standard deviations were estimated using linear least-squares error analysis with uniform weighting of the data points.[38]

Other Physical Measurements. All measurements were made under anaerobic conditions. NMR spectra were recorded on Bruker AM-500N and Varian Mercury 400 spectrometers. Infrared spectra were otained in KBr pellets and measured with a Nicolet Nexus 470 FT-IR spectrometer. Absorption spectra were determined with a Varian Cary 50 Bio spectrophotometer at 298 K.

In the sections that follow, complexes are designated as in Chart 1.

Results and Discussion

Reactions with Arsenite Esters. In this work, the first experiments with arsenic substrates involved As^{III} esters, including $(EtO)_3As$ and two cyclic esters (cf Experimental Section). Equimolar reaction systems of the esters and $[MoO_2(bdt)_2]^{2-}$, intended as an analogue of the (possibly protonated) $Mo^{VI}O_2$ active site of the oxidized enzyme,[31,41] in acetonitrile for ca. 8 h resulted in ligand substitution rather than oxo transfer and 70−80% conversion to $[As(bdt)_2]^{1-}$. When conducted on a preparative scale with $(EtO)_3As$, the Et_4N^+ salt was obtained in (nonoptimized) 26% yield. The overall process is described by reaction 9 (Figure 1) in which the Mo^{VI} product is formulated by analogy to $[Mo_2O_4(OCH_2CH_2OMe)_6]^{2-}$.[42] $(Et_4N)[As(bdt)_2]$ is isomorphous with the corresponding antimony compound,[43] and the anions are isostructural. The structure and metric features of $[As(bdt)_2]^{1-}$ are shown in Figure 2. The anion has a distorted trigonal bipyramidal stereochemistry with atoms S2 and S4 in axial positions, the stereochemically active lone pair in an equatorial position, and an AsS_4 unit with C_{2v} symmetry. The angles $S_{ax}-As-S_{ax}$ = 166.35(4)° and $S_{eq}-As-S_{eq}$ = 106.48(3)° with mean bond lengths $As-S_{ax}$ = 2.51 Å and $As-S_{eq}$ = 2.26 Å. Analogous results were obtained with $[WO_2(bdt)_2]^{2-}$. This unexpected ligand transfer reaction implies a requirement for oxoarsenic substrates in As^{III}/As^{V} conversions by

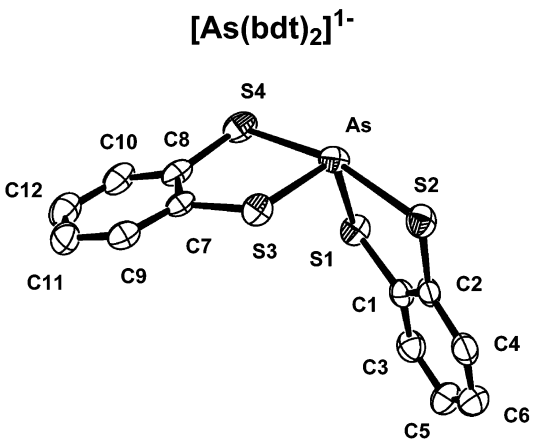

As-S(1)	2.256(2)	As-S(2)	2.498(2)
As-S(3)	2.263(2)	As-S(4)	2.512(2)
S(1)-C(1)	1.768(5)	S(2)-C(2)	1.742(5)
S(3)-C(7)	1.760(5)	S(4)-C(8)	1.737(6)
S(1)-As-S(2)	86.28(5)	S(1)-As-S(3)	106.48(5)
S(1)-As-S(4)	85.40(5)	S(2)-As-S(3)	85.46(7)
S(2)-As-S(4)	166.36(5)	S(3)-As-S(4)	86.56(7)
C(1)-S(1)-As	106.4(2)	C(2)-S(2)-As	101.2(2)
C(7)-S(3)-As	107.0(2)	C(8)-S(4)-As	100.8(2)

dihedral angle of chelate rings 85.3(1)

Figure 2. Structure of $[As(bdt)_2]^{1-}$ as the Et_4N^+ salt showing 50% probability ellipsoids, the atom labeling scheme, and selected bond distances (Å) and angles (deg).

(38) Clifford, A. A. *Multivariate Error Analysis*; Halsted Press: New York, 1973.

(39) Lim, B. S.; Sung, K.-M.; Holm, R. H. *J. Am. Chem. Soc.* **2000**, *122*, 7410−7411.
(40) Sung, K.-M.; Holm, R. H. *Inorg. Chem.* **2000**, *39*, 1275−1281.
(41) Conrads, T.; Hemann, C.; George, G. N.; Pickering, I. J.; Prince, R. C.; Hille, R. *J. Am. Chem. Soc.* **2002**, *124*, 11276−11277.
(42) Turova, N. Y.; Kessler, V. G.; Kucheiko, S. I. *Polyhedron* **1991**, *22*, 2617−2628.
(43) Wegener, J.; Kirschbaum, K.; Giolando, D. M. *J. Chem. Soc., Dalton Trans.* **1994**, 1213−1218.

Table 2. Kinetics Data for the Reaction Systems $[MIV(O\text{-}p\text{-}C_6H_4X)(S_2C_2Me_2)_2]^{1-}$/$Ph_3AsQ$ (M = Mo, W; Q = O, S) in Acetonitrile Solutions

complex	substrate	k_2 ($M^{-1}s^{-1}$) (298 K)		W/Mo reactivity ratio[b]	$\Delta H^{\ddagger}$ (kcal/mol)		$\Delta S^{\ddagger}$ (eu)	
		M = Mo	M = W		M = Mo	M = W	M = Mo	M = W
$[M(O\text{-}p\text{-}C_6H_4Me)(S_2C_2Me_2)_2]^{1-}$	Ph_3AsO	$2.3(1) \times 10^{-2}$	1.8(2)	78	7.3(2)	9.8(3)	−42(1)	−26(2)
	Ph_3AsS	$2.5(2) \times 10^{-1}$	4.1(3)	16	4.9(1)	6.9(5)	−45(2)	−32(4)
$[M(O\text{-}p\text{-}C_6H_4OMe)(S_2C_2Me_2)_2]^{1-}$	Ph_3AsO	$2.4(2) \times 10^{-2}$	1.9(2)	79	7.3(3)	9.8(3)	−40(3)	−25(1)
	Ph_3AsS	$2.6(1) \times 10^{-1}$	4.8(3)	18	4.9(2)	6.7(5)	−45(2)	−33(4)
$[M(OPh)(S_2C_2Me_2)_2]^{1-}$	Ph_3AsO	$2.8(1) \times 10^{-2}$	3.1(1)	111	7.2(3)	9.3(3)	−39(2)	−26(1)
	Ph_3AsS	$2.9(1) \times 10^{-1}$	6.7(1)	23	4.8(3)	6.6(5)	−44(4)	−32(3)
	Ph_3SbS	$5.5(1) \times 10^{-2}$	1.4(1)	25	6.0(2)	8.8(2)	−44(3)	−28(2)
$[M(O\text{-}p\text{-}C_6H_4Br)(S_2C_2Me_2)_2]^{1-}$	Ph_3AsO	$3.7(1) \times 10^{-2}$	6.8(2)	184				
	Ph_3AsS	$5.2(2) \times 10^{-1}$	22.7(3)	44				
$[M(O\text{-}p\text{-}C_6H_4COMe)(S_2C_2Me_2)_2]^{1-}$	Ph_3AsO	$6.0(3) \times 10^{-2}$	9.8(1)	163	6.3(2)	9.1(3)	−39(3)	−25(2)
	Ph_3AsS	$7.5(2) \times 10^{-1}$	66.7(4)	89	4.6(1)	6.4(5)	−44(3)	−29(4)
$[M(O\text{-}p\text{-}C_6H_4CN)(S_2C_2Me_2)_2]^{1-}$	Ph_3AsO	*a*	25.2(3)			8.8(2)		−25(2)
	Ph_3AsS	*a*	228(4)			6.1(5)		−27(4)

[a] Mo complex could not be prepared. [b] k_2^W/k_2^{Mo}.

oxo transfer, a matter supported by the reactivity of Ph_3AsO in the systems which follow.

Reaction Systems for Oxo and Sulfido Transfer. This investigation centers on reactions 7 and 8, which are implemented by the systems **1** or **2**/Ph_3AsO and **1** or **2**/Ph_3AsS in acetonitrile. Complexes **1a**[1] and **2a**[40] have isostructural, practically isometric square pyramidal structures with indistinguishable mean M−S distances (2.32 Å), dihedral angles between chelate rings (126−127°), and displacements of the metal atom from the S_4 plane toward the axial phenoxide ligand (0.78−0.79 Å). Axial bond distances (Mo−O 1.898(5) Å, W−O 1.861(3) Å) differ by ca. 0.03 Å. The substrates are simple tetrahedral molecules with nearly identical bond angles and bond lengths As−S (2.079(4), 2.095(5) Å)[44,45] and As−O (1.65, 1.641(3) Å)[46] that differ by 0.44−0.45 Å, including *p*-chloro derivatives.[47] The gas-phase As−O bond dissociation energy of Ph_3AsO calculated from other thermodynamic data is 103 kcal/mol, essentially the same as that for $MoOCl_4$ (101 kcal/mol).[48] Hoff and co-workers[28] have estimated from gas-phase and solution enthalpies that the As−S bond energy in Ph_3AsS is 70 kcal/mol. The two substrates are, therefore, stereochemically congruous but differ in bond length, bond strength, and presumably, basicity (vide infra).

The reaction systems are suitable to address the determinations (i) and (ii) specified above. Rate constants at 298 K were measured for five Mo^{IV} (**1a**−**1e**) and six W^{IV} (**2a**−**2f**) complexes, each with both Ph_3AsO and Ph_3AsS as substrates, in acetonitrile solutions. Complexes differ in terms of the para-substituent (X′ = H, Me, OMe, Br, COMe, CN) of the axial phenolate ligand. Activation parameters were determined for four Mo^{IV} and five W^{IV} systems with both substrates. Kinetic parameters are collected in Table 2.

Oxo Transfer. Reactions 7a (M = Mo) and 7b (M = W) are depicted schematically in Figure 1. Spectral changes over the course of typical reactions are shown in Figure 3. For the Mo^{IV} system **1a**/Ph_3AsO, equimolar components at the millimolar concentration level resulted in no appreciable reaction over ca. 8 h, after which decomposition occurred. The use of ≳5 equiv of substrate resulted in nearly complete reaction in 2 h. In this system, a tight isosbestic point is observed at 523 nm. The bands at 576 and 830 nm increase in intensity with time and arise from Mo^V complex **7**. The reaction proceeds by relatively slow atom transfer to form

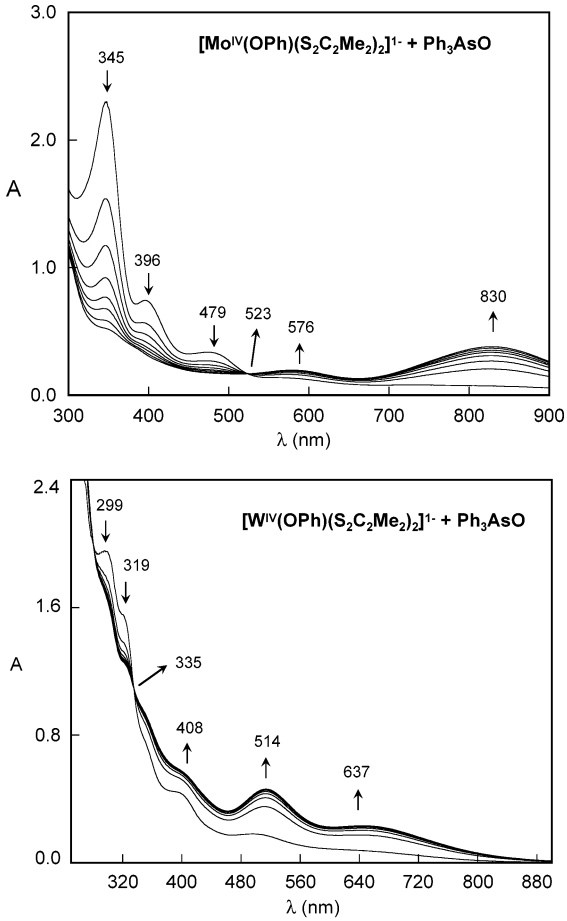

Figure 3. UV/visible spectra for the reaction systems $[M(OPh)(S_2C_2Me_2)_2]^{1-}$/$Ph_3AsO$ (M = Mo, W) in acetonitrile at 298 K. The systems intially contained 1.88 mM Mo^{IV} and 25.0 mM Ph_3AsO (upper), and 1.50 mM W^{IV} and 1.88 mM Ph_3AsO (lower). In these and other spectra, arrows indicate changes in absorbance with time; peak maxima and isosbestic points are indicated.

(44) Boorman, P. M.; Codding, P. W.; Kerr, K. A. *J. Chem. Soc., Dalton Trans.* **1979**, 1482−1485.
(45) Narayana, S. V. L.; Shrivastava, H. N. *Acta Crystallogr.* **1981**, *B37*, 1186−1189.
(46) Shao, M.; Jin, X.; Tang, Q.; Huang, Y. *Tetrahedron Lett.* **1982**, *23*, 5343−5346.
(47) Belsky, V. K.; Zavodnik, V. E. *J. Organomet. Chem.* **1984**, *265*, 159−165.
(48) Holm, R. H.; Donahue, J. P. *Polyhedron* **1993**, *12*, 571−589.

$Mo^{VI}O$ complex **3** followed by a rapid internal redox reaction to produce **7** and the phenoxyl radical, which is quenched to phenol by hydrogen atom abstraction. The final spectrum is that of **7** (blue-violet) measured separately. The situation is closely analogous to the reactions of **1a** with S-oxides and has been analyzed by the same procedure, including spectrophotometric demonstration of the conversion **3** → **7** and demonstration of the formation of phenol.[1] Despite numerous attempts, we have never been able to isolate pure samples of complex **3** and related species such as $[Mo^{VI}O_2(S_2C_2R_2)_2]^{2-}$ (R = Ph, CO_2Me). The requirement of a more electronegative dithiolene ligand, as in $[MoO(OSiR_3)(bdt)_2]^{1-}$,[49] $[MoO_2(bdt)_2]^{2-}$,[34] and $[MoO_2(S_2C_2(CN)_2)_2]^{2-}$,[50] allowing isolation and structure determination, makes evident the susceptibility of monooxo and dioxo Mo^{VI} dithiolenes to internal reduction in an electron-rich environment. The related $W^{VI}O$ complexes **4** are sufficiently stable for isolation;[2,14] consequently, tungsten-mediated oxo-transfer reactions are free of the complication of a follow-up redox process.

The W^{IV} system **2a**/Ph_3AsO with equimolar components proceeded to near-completion within 3 h and develops a clean isosbestic point at 335 nm and bands at 408, 514, and 637 nm that increase in intensity as the reaction progresses. The final spectrum is that of the $W^{VI}O$ complex **4a**, which is readily distinguished from that of $[W^{V}O(S_2C_2Me_2)_2]^{1-}$. Reactions 7 follow the second-order rate law eq 10 (Q = O). Kinetics parameters are collected in Table 2. Values for **4a** are in excellent agreement with an earlier determination.[2] For some six complexes, rate constants k_2 define the ranges

$$\frac{-d[M^{IV}]}{dt} = k_2[M^{IV}][Ph_3AsQ] \qquad (10)$$

0.023−0.060 M^{-1} s^{-1} for molybdenum and 1.8−9.8 M^{-1} s^{-1} for tungsten, with the reactivity ratios k_2^W/k_2^{Mo} = 78−184. Activation parameters were evaluated for eight systems. Values of $\Delta S^{\ddagger}$ are large and negative for both molybdenum- and tungsten-mediated reactions, consistent with an associative transition state.

Sulfido Transfer. Reactions 8a and 8b are described in Figure 1. The spectrophotometric time courses of two typical reactions are presented in Figure 4. The Mo^{IV} system **1a**/Ph_3AsS displays a well-defined isosbestic point at 368 nm and bands at 459, 577, and 731 nm that increase in intensity with time. The final spectrum is that of disulfido-bridged complex **8**, previously isolated in low yield from the heterogeneous reaction of $[Mo(CO)_2(S_2C_2Me_2)_2]$ and Na_2S in acetonitrile and structurally characterized.[35] Sulfur atom transfer occurs, presumably generating $Mo^{VI}S$ complex **5a** which has not been directly detected, followed by internal reduction. This and other complexes **5** are too unstable to isolate, another manifestation of the reducibility of Mo^{VI} complexes containing electron-rich dithiolene ligands. This complication is absent in the analogous tungsten system.

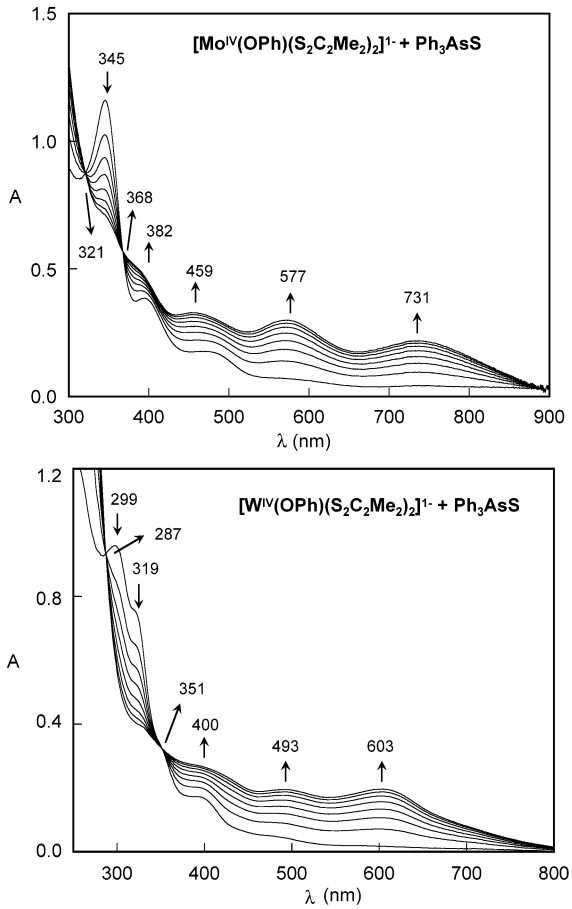

Figure 4. UV/visible spectra for the reaction systems $[M(OPh)(S_2C_2Me_2)_2]^{1-}$/$Ph_3AsS$ (M = Mo, W) in acetonitrile at 298 K. The systems intially contained 0.94 mM Mo^{IV} and 5.00 mM Ph_3AsS (upper), and 0.75 mM W^{IV} and 0.75 mM Ph_3AsS (lower).

Prior to the kinetics runs, the complexes **6** were generated in situ by reaction 8b. The formation of $W^{VI}S$ complexes was assured by comparison of methyl chemical shifts with that of **6a**, which has been prepared and whose X-ray structure has been determined.[14] The equimolar W^{IV} reaction system **2a**/Ph_3AsS reacts immediately and generates a tight isosbestic point at 351 nm and bands at 400, 493, and 603 nm that intensify as the reaction proceeds. The final spectrum is that of $W^{VI}S$ complex **6a**. The reactions 8 are described by rate law 10 (Q = S). The faster reaction rates necessitated stopped-flow measurements, illustrated in Figure 5 for the system **2c**/Ph_3AsS. Rate constants k_2 are 0.25−0.75 $M^{-1}s^{-1}$ for molybdenum and 4.1−66.7 $M^{-1}s^{-1}$ for tungsten with reactivity ratios 16−89. Eyring plots for the reactions of complexes **1c** and **2c**, shown in Figure 5, display the strict linear behavior found in these and other systems. As for molybdenum-mediated sulfido transfer, activation entropies accord with an associative transition state. These are the first kinetics results for metal-mediated sulfido transfer reactions.

Reactivity Ratios. The ratios in Table 2 demonstrate that in every case $k_2^W > k_2^{Mo}$ and that for a given complex the ratio is always larger for Ph_3AsO than Ph_3AsS. The results provide one more proof that at parity of structure and ligation oxo transfer from substrate to metal ($M^{IV} \rightarrow M^{VI}O$) is faster with tungsten and that to substrate from metal ($M^{VI}O \rightarrow M^{IV}$) is faster with molybdenum. Prior examples of this result have

(49) Donahue, J. P.; Goldsmith, C. R.; Nadiminti, U.; Holm, R. H. *J. Am. Chem. Soc.* **1998**, *120*, 12869−12881.
(50) Das, S. K.; Chaudhury, P. K.; Biswas, D.; Sarkar, S. *J. Am. Chem. Soc.* **1994**, *116*, 9061−9070.

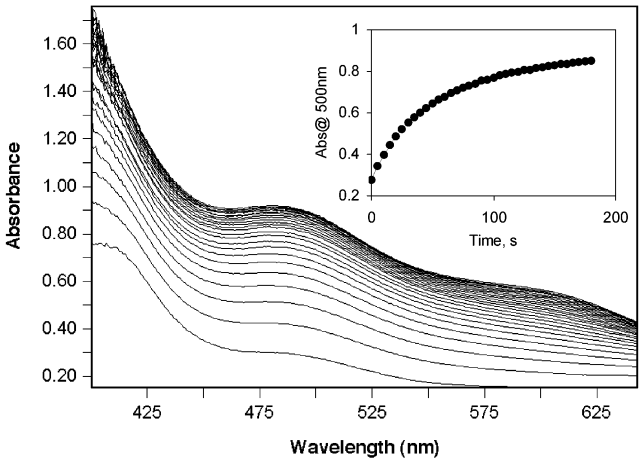

Figure 5. Stopped-flow time-resolved UV/visible spectra of the reaction system $[W(O\text{-}p\text{-}C_6H_4COMe)(S_2C_2Me_2)_2]^{1-}$/$Ph_3AsS$ (both at 25 mM) in acetonitrile at 298 K. Spectra were recorded at 5-s intervals. Inset: kinetics trace of the reaction at 500 nm (dots) superimposed with a second-order fit ($k_2 = 66.7\ M^{-1}\ s^{-1}$).

been observed for both synthetic and enzymic systems.[2,4,51] The present results provide the first demonstration that the same regularity applies to sulfido transfer. Both sets of results reveal a kinetic metal effect on atom transfer.

Atom Donor/Acceptor Series. We have introduced a thermodynamic series for oxo transfer based on the enthalpies or free energies of the reaction $X + {}^1/_2O_2 \rightarrow XO$, allowing an ordering of molecules X/XO on the basis of their affinity for acceptance or donation of an oxygen atom.[48] In the absence of thermodynamic data, certain partial series may be constructed on the basis of qualitative observations of reactivity. In the systems following, reactions were performed at ambient temperature. For example, reactions 11 (1:1) and 12 (5:1), with the indicated $M^{VI}O_2/W^{IV}$ molar ratios and involving previously reported M = $Mo^{VI,IV}$ [34,49] and $W^{VI,IV}$ [13,52] complexes, proceed to at least 80% completion in acetonitrile in ca. 1 h. The reactions were monitored by ^1H NMR, which distinguishes reactants and products, especially **2a** (δ_{Me} 2.61) and **4a** (δ_{Me} 2.19). In these reactions, the $[MO_2(bdt)_2]^{2-}$ complexes are stronger oxo donors than the $W^{VI}O$ dithiolene product. No reaction occurs between $[MO(bdt)_2]^{2-}$ or **2a** and Ph_3PO. Further, reaction 13 occurs to ca. 70% completion within 1 h, confirming the expected result that $Mo^{VI}O_2$ is a stronger donor than $W^{VI}O_2$ in the bdt series. Reaction 14 proceeds completely to the right with excess Ph_3As; therefore, $[MoO_2(bdt)_2]^{2-}$ is a stronger oxo donor than Ph_3AsO. The system $[WO(bdt)_2]^{2-}$/excess Ph_3AsO was not well-behaved. No reaction is observed under the same conditions with $[WO_2(bdt)_2]^{2-}$, nor with any W^{IV} or $M^{IV}O$ complex and Ph_3PO. On the basis of observations in this and previous work,[1,2,26,34] oxo donor series 15 is formulated, in which only isolable complexes are included and the bracketed entries cannot be ordered with information currently available. As might be expected, the oxo-W^{VI} complexes are relatively weak oxo donors and on the thermodynamic scale have reaction enthalpies in the range $\Delta H = -43$ to -74 kcal/mol. The related W^{IV} complexes are, of course, strong oxo acceptors. Reactions 11−13 are classified as intermetal oxo transfer processes.[5]

$$[W(OPh)(S_2C_2Me_2)_2]^{1-} + [MoO_2(bdt)_2]^{2-} \rightarrow [WO(OPh)(S_2C_2Me_2)_2]^{1-} + [MoO(bdt)_2]^{2-} \quad (11)$$

$$[W(OPh)(S_2C_2Me_2)_2]^{1-} + [WO_2(bdt)_2]^{2-} \rightarrow [WO(OPh)(S_2C_2Me_2)_2]^{1-} + [WO(bdt)_2]^{2-} \quad (12)$$

$$[WO(bdt)_2]^{2-} + [MoO_2(bdt)_2]^{2-} \rightarrow [WO_2(bdt)_2]^{2-} + [MoO(bdt)_2]^{2-} \quad (13)$$

$$[MoO_2(bdt)_2]^{2-} + Ph_3As \rightarrow [MoO(bdt)_2]^{2-} + Ph_3AsO \quad (14)$$

$$Me_3NO > (CH_2)_4SO > [MoO_2(bdt)_2]^{2-} > \{Ph_3AsO > [WO_2(bdt)_2]^{1-}\} > [WO(OPh)(S_2C_2Me_2)_2]^{1-} > Ph_3PO > Ph_2MePO \quad (15)$$

A thermodynamic scale for sulfur atom transfer has not yet been devised. Reaction 16 with excess phosphine proceeds rapidly and nearly completely, showing that **6a** is a better sulfur atom donor than Ph_3PS. With this and other information,[26,28] the short sulfido donor series 17 is formulated.

$$[WS(OPh)(S_2C_2Me_2)_2]^{1-} + Ph_3P \rightarrow [W(OPh)(S_2C_2Me_2)_2]^{1-} + Ph_3PS \quad (16)$$

$$Ph_3SbS > Ph_3AsS > Ph_2MeAsS > [WS(OPh)(S_2C_2Me_2)_2]^{1-} > Ph_3PS > Ph_2MePS \quad (17)$$

Reaction Pathway. To address the question of the pathway of oxo transfer mediated by bis(dithiolene) molybdenum and tungsten complexes, the reactions 18 were examined in some detail.[2,3] In common with reactions 7 and 8, these are second-order with large negative activation entropies and associative transition states. Axial (X′) and in-plane (Y) ligand substituents were independently varied, affording linear free energy relationships including $\Delta G^{\ddagger}$ versus σ_p. The most important finding was that electron-withdrawing groups (EWGs) accelerate rates and electron-donating groups (EDGs) decrease rates, relative to the system with X′ = Y = H, in reactions with constant substrate. It was concluded that the probable pathway proceeds through an early transition state with substantial XO···W bond-making character. This description is thought to apply to the

$$[W^{IV}(OC_6H_4\text{-}p\text{-}X')(S_2C_2(C_6H_4\text{-}p\text{-}Y)_2)_2]^{1-} + (CH_2)_4SO \rightarrow [W^{VI}O(OC_6H_4\text{-}p\text{-}X')(S_2C_2(C_6H_4\text{-}p\text{-}Y)_2)_2]^{1-} + (CH_2)_4S \quad (18)$$

(51) Tucci, G. C.; Donahue, J. P.; Holm, R. H. *Inorg. Chem.* **1998**, *37*, 1602−1608.
(52) Ueyama, N.; Oku, H.; Nakamura, A. *J. Am. Chem. Soc.* **1992**, *114*, 7310−7311.

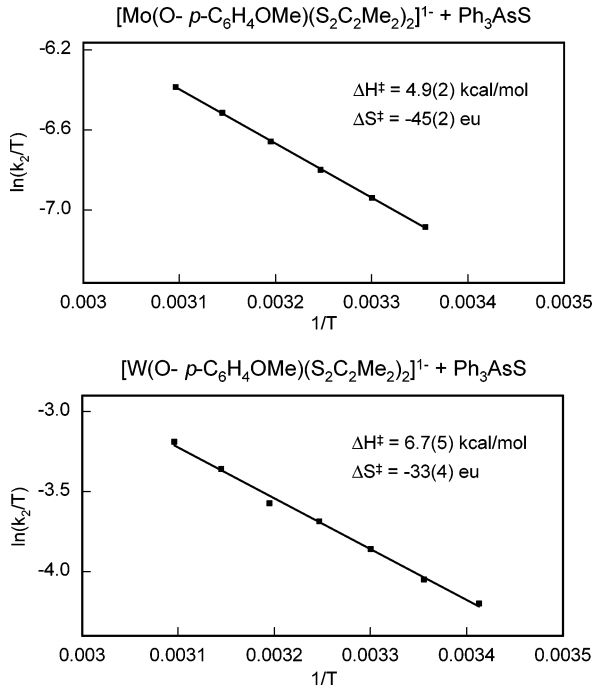

Figure 6. Eyring plots for two sulfido-transfer systems in acetonitrile based on $[M(O\text{-}p\text{-}C_6H_4OMe)(S_2C_2Me_2)_2]^{1-}$ with M = Mo^{IV} (upper) and W^{IV} (lower).

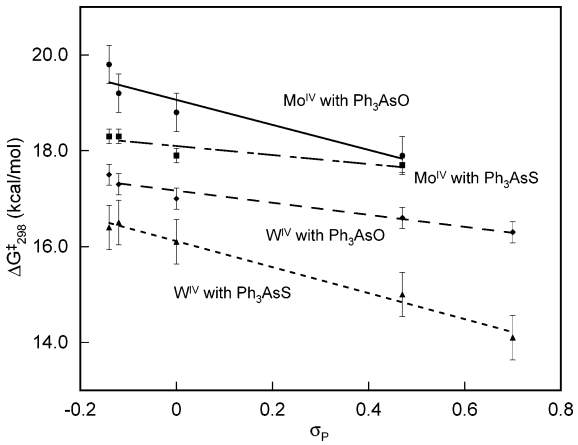

Figure 7. Linear free-energy relationships between the activation free energies and substituent constants for reactions 7 and 8. Correlation coefficients and slopes (kcal/mol): Mo^{IV}/Ph_3AsO, $R = 0.934$, −2.61; Mo^{IV}/Ph_3AsS, $R = 0.894$, −0.94; W^{IV}/Ph_3AsO, $R = 0.972$, −1.26; W^{IV}/Ph_3AsS, $R = 0.994$, −2.71.

corresponding molybdenum systems which also display second-order kinetics and an associative pathway.

An analogous but less extensive approach to the reaction pathway was applied to reactions 7 and 8 utilizing Mo^{IV} complexes **1a**−**1c** and **1e** and W^{IV} complexes **2a**−**2c**, **2e**, and **2f**. The data in Table 2 may be considered in terms of the reaction sets $[M^{IV}X'/Q]$ in which the metal M = Mo or W, para substituent X′ of the axial phenolate, and substrate containing Q = O or S are independently varied and other components of the set are held constant. Activation parameters reveal that $|T\Delta S^{\ddagger}| > \Delta H^{\ddagger}$ except for the set $[W^{IV}X'/O]$; these values are apportioned such that overall $\Delta H^{\ddagger}$ is ca. 30−60% of $\Delta G^{\ddagger}$. Consequently, neither enthalpy nor entropy factors predominate. Certain features of the activation parameters emerge across the reaction sets.

(i) Variable M, constant Q and X′: $\Delta H^{\ddagger}_W > \Delta H^{\ddagger}_{Mo}$, $|T\Delta S^{\ddagger}|_{Mo} > |T\Delta S^{\ddagger}|_W$. The faster rates with tungsten at constant substrate, expressed by the reactivity ratios 78−184 (Q = O) and 16−89 (Q = S), are due mainly to smaller (less negative) activation entropies which tend to compensate the 2−3 kcal/mol higher activation enthalpies.

(ii) Variable Q, constant M and X′: $\Delta H^{\ddagger}_M{}^O > \Delta H^{\ddagger}_M{}^S$, $|T\Delta S^{\ddagger}|_M{}^S > |T\Delta S^{\ddagger}|_M{}^O$. Smaller activation enthalpies are mainly responsible for faster rates with Ph_3AsS than those with Ph_3AsO. The constant order of activation entropies (although small differences) may reflect a large extent of solvation of the more polar Ph_3AsO in achieving the transition state.

(iii) Variable X′, constant M and Q: $\Delta H^{\ddagger}$ and $|T\Delta S^{\ddagger}|$ are essentially constant contributors to $\Delta G^{\ddagger}$ within each set; for example, in [WX′/O] and [WX′/S] $\Delta H^{\ddagger}$ is 55−57% and 41−43%, respectively. The effects are manifested as the linear free energy relationships $\Delta G^{\ddagger}$ versus σ_p in Figure 7. In these plots, we have used relatively recent substituent constants for $-CH_3$ (−0.14) and $-OCH_3$ (−0.12)[53] that are nearly the same. The negative slopes convey that EWGs groups accelerate rates in the four reaction sets [MX′/O] and [MX′/S]. The effect is best developed in the set [WX′/S], which has the largest slope and five reaction components.

Concerning feature i, the same trend in parameters has been observed in the systems **1a**, **2a**/$(CH_2)_4SO$, for which $\Delta S^{\ddagger}$ = −39 (Mo) and −33 (W) eu.[1,2] In this sense, the behavior of the two oxo donor substrates is consistent. The main contributors to $\Delta S^{\ddagger}$ are rearrangement of the M^{IV} complex from square pyramidal to a distorted octahedral configuration like that of **2a** or **6a** and concomitant substrate binding and solvation changes. The structures of molybdenum complexes **3** and **5**, while unavailable, surely will be isostructural with the corresponding tungsten complexes. The smaller values of $\Delta S^{\ddagger}_W$ may reflect a less solvated transition state, perhaps with more tightly bound substrate.

Feature ii points to a differential $\Delta H^{\ddagger}$ component to rate differences in the systems [MX′/O] versus [MX′/S], which could reflect strengths of M···$QAsPh_3$ bond-making or As-Q bond-weakening in the transition state. As one measure of basicity, we note that Ph_3AsO is readily protonated and that As−O bond lengths in various $(Ph_3AsOH)^+$ salts (1.69−1.73 Å)[54−58] exceed that in Ph_3AsO by ca. 0.04−0.08 Å. We are unaware of structural information for protonated Ph_3AsS. Attachment of either substrate to an electrophilic center, as in a transition state, is predicted to weaken the Q-As bond. The only available measure of relative basicity

(53) Carey, F. A.; Sundberg, R. J. *Advanced Organic Chemistry*; Kluwer Academic/Plenum Publishers: New York, 2000; Part A, p 208.
(54) Ferguson, G.; Macaulay, E. W. *Chem. Commun.* **1968**, 1288−1290.
(55) March, F. C.; Ferguson, G. *J. Chem. Soc., Dalton Trans.* **1975**, 1381−1384.
(56) Jones, P. G.; Olbrich, A.; Schwarzmann, E. *Acta Crystallogr.* **1988**, *C44*, 2201−2202.
(57) Massabni, A. C.; Nascimento, O. R.; Halvorson, K.; Willett, R. D. *Inorg. Chem.* **1992**, *31*, 1779−1784.
(58) Batt, R. V.; Bullivant, D. P.; Elkington, K. E.; Hill, S. E.; Hilton, J.; Houghton, T. J.; Hovell, M.; Wallwork, S. C. *Polyhedron* **1998**, *17*, 2173−2178.

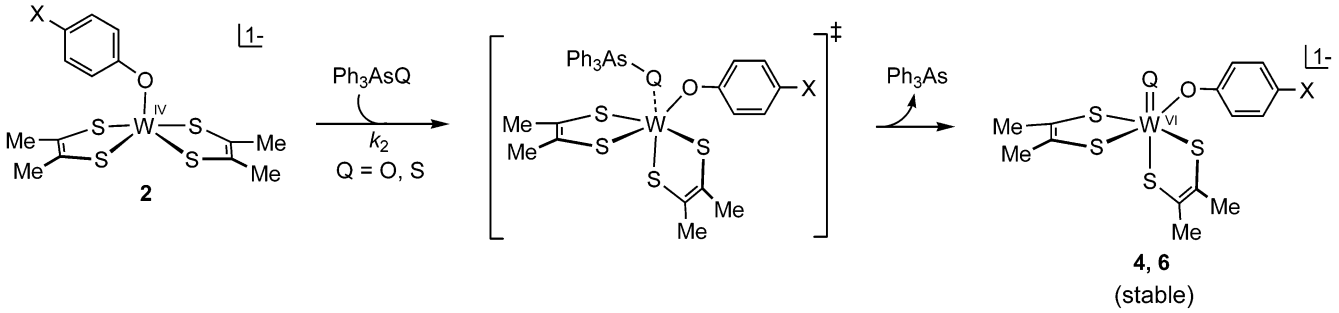

Figure 8. Simple depiction of the proposed reaction pathway for the atom transfer reactions of tungsten complexes **2** with Ph_3AsQ to produce oxo complexes **4** and sulfido complexes **6**. The associative transition state is proposed to involve Q···W bond-making and Q−As bond weakening. Systems based on the Mo^{IV} complexes **1** are expected to have an analogous pathway.

in solution indicates that Ph_3AsO (pK_a 1.25) is a stronger proton base than Ph_3AsS (pK_a −2.91) in acetic anhydride.[59]

Feature iii parallels the behavior of the reactions 18. We suggest a pathway, depicted in Figure 8, which implicates a transition state with certain probable characteristics. Its structure is expected to resemble the distorted cis-octahedral configurations of oxo and sulfido reaction products **4a**[2] and **6a**,[14] respectively. Appreciable M···QAsPh_3 bond making is consistent with the linear free energy behavior in Figure 7. Here, EWGs would make the M^{IV} center relatively more electrophilic, which should promote substrate binding and therewith lower $\Delta G^{‡}$ for formation of an associative transition state. Some degree of Q−As bond weakening reflects the ca. 30 kcal/mol lower bond energy of the sulfide than that of the oxide and in this interpretation is a contributor to the faster reaction rates of the former substrate. The bond weakening feature was not detected in reaction 18, where the substrate is constant. Bond strengths may contribute to the ca. 10^6 times larger rate constant for the reaction of molybdenum complex **1a** with Me_3NO (D = 61 kcal/mol)[1,60] than that of **1a** with $(CH_2)_4SO$ (D = 86−87 kcal/mol).[48,61] More detailed discussions of the factors which underlie the proposed reaction pathway together with depictions of reaction coordinates are presented elsewhere.[2,3]

Summary. The following are the principal results and conclusions of this investigation, whose primary purpose has been determination of the relative kinetics of oxygen and sulfur atom transfer in the form of reactions 7 and 8 in acetonitrile with the homologous substrates Ph_3AsO and Ph_3AsS. Rate constants refer to 298 K.

(1) All oxo and sulfido transfer reactions follow second-order kinetics with associative transition states connoted by large negative activation entropies: $\Delta S^{‡}_{Mo} = -39$ to -45 eu, $\Delta S^{‡}_{W} = -25$ to -33 eu.

(2) Sulfido transfer to a Mo^{IV} or W^{IV} center is always faster than oxo transfer at parity of ligand by a nearly constant factor: $k_2^S/k_2^O = 10-14$.

(3) Oxo or sulfido transfer to a W^{IV} center is always *faster* than to a Mo^{IV} center at parity of ligand and substrate: $k_2^W/k_2^{Mo} = 78-184$ (oxo), 16−89 (sulfido).

(4) Increasing electron-withdrawing capacity of group X′ in molybdenum or tungsten complexes $[M^{IV}(O\text{-}p\text{-}C_6H_4X')(S_2C_2Me_2)_2]^{1-}$ increases the rate of sulfido or oxo transfer.

(5) The proposed transition state involves a significant component of bond making between substrate and W^{IV} (or Mo^{IV}) center and concomitant As−O or As−S bond weakening. A common reaction pathway having the characteristics in 1 appears operative in oxo and sulfido transfer reactions of bis(dithiolene)Mo^{IV} and -W^{IV} complexes.[1−3]

In assessing the findings of this investigation, it should be borne in mind that comparative rate effects are small and that the main conclusions are based on trends rather than on quantitative differences. In this regard, note the results for Ph_3SbS (Table 2), a known sulfur atom donor[26,27] with a stereochemistry strictly analogous to Ph_3AsQ.[62] With the Mo^{IV} and W^{IV}, this substrate reacts more slowly by a factor of 5 than does Ph_3AsS, whose bond energy of 70 kcal/mol is only 3 kcal/mol more than that estimated for Ph_3SbS.[28] We are uncertain as to the cause of this small but unexpected rate reversal.

Acknowledgment. This research was supported by NSF grants CHE 0237419 at Harvard University and 0111202 at Tufts University. We thank Dr. J. Jiang for a crystal structure determination and Dr. S. C. Lee for useful discussions.

Supporting Information Available: X-ray crystallographic files in CIF format for the structure determination of the compound in Table 1. This material is available free of charge via the Internet at http://pubs.acs.org.

IC040087F

(59) Gel'fond, A. S.; Galyametdinov, Yu. G.; Khalikova, N. A.; Chernokal'skii, B. D. *Zh. Obshch. Khim.* **1976**, *46*, 2077−2082.
(60) Acree, W. E., Jr.; Tucker, S. A.; Ribeiro da Silva, M. D. M. C.; Matos, M. A. R.; Gonçalves, J. M.; Ribeiro da Silva; Pilcher, G. *J. Chem. Thermodyn.* **2000**, *27*, 391−398.
(61) Jenks, W. S.; Matsunaga, N.; Gordon, M. *J. Org. Chem.* **1996**, *61*, 1275−1283.
(62) Pebler, J.; Weller, F.; Dehnicke, K. *Z. Anorg. Allg.Chem.* **1982**, *492*, 139−147.